Taylor & Francis
Taylor & Francis Group

Journal of Adhesion Science and Technology

ISSN: 0169-4243 (Print) 1568-5616 (Online) Journal homepage: http://www.tandfonline.com/loi/tast20

Fabrication of optically clear acrylic pressure–sensitive adhesive by photo-polymerization: UV-curing behavior, adhesion performance, and optical properties

Soyon Kim , Seung-Woo Lee , Dong-Hyuk Lim , Ji-Won Park , Cho-Hee Park & Hyun-Joong Kim

To cite this article: Soyon Kim , Seung-Woo Lee , Dong-Hyuk Lim , Ji-Won Park , Cho-Hee Park & Hyun-Joong Kim (2013) Fabrication of optically clear acrylic pressure–sensitive adhesive by photo-polymerization: UV-curing behavior, adhesion performance, and optical properties, Journal of Adhesion Science and Technology, 27:20, 2177-2190, DOI: 10.1080/01694243.2013.763480

To link to this article: https://doi.org/10.1080/01694243.2013.763480

Published online: 24 Jan 2013.

Journal of Adhesion Science and Technology, 2013
Vol. 27, No. 20, 2177–2190, http://dx.doi.org/10.1080/01694243.2013.763480

Taylor & Francis
Taylor & Francis Group

Fabrication of optically clear acrylic pressure–sensitive adhesive by photo-polymerization: UV-curing behavior, adhesion performance, and optical properties

Soyon Kim[a], Seung-Woo Lee[a], Dong-Hyuk Lim[a], Ji-Won Park[a], Cho-Hee Park[a]
Hyun-Joong Kim[a,b]*

[a]*Laboratory of Adhesion & Bio-Composites, Program in Environmental Materials Science, Seoul National University, Seoul 51-921, Republic of Korea;* [b]*Research Institute for Agriculture & Life Science, Seoul National University, Seoul 151-921, Republic of Korea*

(*Received 3 November 2012; accepted 3 January 2013*)

Acrylic pressure–sensitive adhesives (PSAs) with 2-phenoxy ethyl acrylate (PEA) were polymerized using UV-curing technology. This study examined the effects of PEA content and UV dose. The photo-polymerization behavior of the pre-polymer was examined by viscosity measurements, real-time Fourier transform infrared spectroscopy, and photo-differential scanning calorimetry. The curing behaviors of the acrylic PSAs were investigated by shrinkage test, a modular advanced rheometer system, and gel content. differential scanning calorimetry and Advanced Rheometric Expansion System were used to characterize the acrylic PSAs. Adhesion performances were measured by probe tack, peel strength, and shear adhesion failure temperature. The optical properties of acrylic PSAs were examined by UV–visible spectroscopy and prism coupler. The PEA content had a larger effect on improving the optical properties, than did the UV dose. The transmittances of the acrylic PSAs with <75% PEA were >95%. The refractive indices of the acrylic PSAs increased with increasing PEA content, due to its high refractive index, >1.5, which affected the overall refractive indices, particularly in the visible region.

Keywords: acrylic PSAs; phenoxy ethyl acrylate; adhesion performance; UV-curing behavior; optical properties

1. Introduction

Pressure–sensitive adhesive (PSA) tapes composed of acrylic copolymers have been extensively utilized in various applications including packaging, printing, electrical insulation, and automobile parts. In general, the PSA properties (tack, peel adhesion, and holding power) of acrylic adhesives have been controlled by blending tackifiers or dissimilar polymers, by adjusting molecular weight and its distribution, and also by copolymerization with a polar monomer and by varying the curing system. In recent years, the PSA properties of acrylic adhesive copolymers have been interpreted by considering various factors, such as dynamic mechanical properties, surface tension, and miscibility.[1–5]

Recently, UV-curing technology has been used in crosslinking PSAs, owing to its economical and environmental advantages, with none of the disadvantages associated with

*Corresponding author. Email: hjokim@snu.ac.kr

using a crosslinking agent. UV-curing technology has many benefits, because of its high performance, saving process, and low emission of volatile organic compounds (VOCs).[6] Therefore, UV-curing has attracted considerable attention for use in many applications. UV-curing technology is used for many purposes, such as adhesives, inks, and coatings.

To make UV-curable PSAs, an oligomeric resin, reactive diluents, photoinitiator, and other additives are needed. With this formulation, UV-curable PSAs can be synthesized after a few minutes of UV irradiation. This type of UV-curable PSA also has the advantages of UV-curing technology. The conversion rate of the monomer to polymer is quite high; PSAs can be polymerized in a few minutes. In addition, there is no solvent that can induce the emission of VOCs after polymerization in PSA formulations. Therefore, it has low environmental impact, and can be coated onto surfaces thickly, due to the lack of a solvent that evaporates after the coating process.[7]

Because of this high performance, UV-curable PSAs can have optical applications. Optical PSAs are being used increasingly in areas such as liquid crystal displays, plasma display panels, and organic light emitting diodes, due to increase in optical device production.[8] Optical PSAs should have high contrast, clarity, high refractive index, and good reliability.[9] These properties can be achieved with UV-curing technology. Acrylic PSAs are generally transparent, and show high adhesion performance. The polymerization of acrylic PSAs using UV-curing technology can increase the solid content of PSAs, which will reduce the emission of VOCs from the solvent. Moreover, the coating thickness can be increased, due to high solid content.

In this study, transparent acrylic PSAs with high refractive index were prepared by photo-polymerization using a UV light source. An acrylic monomer containing 2-phenoxy ethyl acrylate (PEA) was used to achieve this property. The UV-curing behaviors of the UV-curable acrylic PSAs, adhesion performance, and optical properties of the PSAs were examined.

2. Experimental

2.1. Materials

Acrylic monomers, including 2-ethyl hexyl acrylate (2-EHA, 99.0% purity, Samchun Pure Chemical Co. Ltd, South Korea), PEA (90.0% purity, Tokyo Chemical Industry, Japan), and acrylic acid (AA, 99.0% purity, Samchun Pure Chemical Co. Ltd, South Korea) were commercially available and used as received. Darocur 2,4,6-trimethylbenzoyl-diphenyl-phosphineoxide (TPO) (TPO, Ciba Chemical Co. Ltd, Germany) was used as the photoinitiator and aluminum acetyl acetonate (AlAcA, Dongsan Chemical, South Korea) was used as the curing agent.

2.2. Photo-polymerization behavior of pre-polymer

2.2.1. Photo-polymerization of pre-polymer

The pre-polymer was synthesized by photo-polymerization from 2-EHA, PEA, and AA using a UV light source. Mixtures of the acrylic monomers and photoinitiator were held in a 500 ml four-necked round-bottom flask equipped with a thermometer, mechanical stirrer, nitrogen gas, and UV spot curing equipment (SP-9-250UB, USHIO INC. System Company, Japan). The main wavelength was 365 nm. The flasks were purged with nitrogen gas for 10 min before photo-polymerization to prevent photoinitiator inhibition by oxygen. The sample was then irradiated with UV light for 1 min, with a further 1 min to stabilize. Polymerization was complete after an additional exposure to UV light for 1 min.

2.2.2. Viscosity

The viscosity of the photo-polymerized pre-polymer was measured using a Brookfield Viscometer (DV-II+) equipped with spindle No. 7 at 25 °C. A 200 ml of the pre-polymer was contained in a cylindrical case with a 500 ml capacity, to reduce the resistance from the surface.

2.2.3. Real-time Fourier transform infrared spectroscopy

The real-time Fourier transform infrared (RTIR) spectra were obtained using an FTIR-6100 (Jasco, Japan) with an attenuated total reference (ATR) accessory. Rapid scan mode was used for high speed measurements. To determine the photo-polymerization behavior of the pre-polymer, UV was irradiated with a 100 mJ/cm^2 intensity for 600 s, and the RTIR spectra were observed for 600 s. UV spot curing equipment (SP-9-250UB, USHIO INC. System Company, Japan) was used as the light source. The spectral range analyzed was 750–4000 cm^{-1}. The data were collected for a 0.964233 cm^{-1} pitch and a time interval of 0.139 s. The photo-polymerization behavior was monitored from the cross section at 810 cm^{-1}, which is the peak of the C=C double bond, for 600 s. All the monomers (10 μm) were dropped onto the ATR crystal and the experiment was held at 25 °C.

2.2.4. Photo-differential scanning calorimetry

The photo-polymerization behavior of 2-EHA and PEA with TPO was measured by differential scanning calorimetry (DSC, Q-1000, TA Instrument, USA) equipped with a photo-calorimetric accessory. The UV light source was a 100 W middle-pressure mercury lamp under nitrogen gas, with an intensity of 70 mW/cm^2 over the spectral range of 300–545 nm. A 3 mg sample was weighed and placed on an open aluminum DSC pan. The temperature was held at 25 °C. The heat released during photo-polymerization was detected.

2.3. UV-curing behavior of acrylic PSAs

2.3.1. Preparation of acrylic PSAs

The photo-polymerized pre-polymer was mixed with AlAcA and an additional TPO, and then coated on 80 μm thick corona-treated polyethylene terephthalate (PET, SKC Co. Ltd, South Korea) films. The pre-polymer was cured using conveyor belt-type UV-curing equipment with a 100 W high pressure mercury lamp. The main wavelength was 365 nm. The UV doses used were 0, 250, 500, 750, and 1000 mJ/cm^2. The UV doses were gauged using an IL 390C Light Bug UV radiometer (International Light, USA).

2.3.2. Modular advanced rheometer system

The UV-curing behaviors of the acrylic PSAs were observed with a HAAKE MARS II Rheometer (Thermo Fisher Scientific Inc., Germany). The viscoelastic moduli of the acrylic PSAs during UV-curing were determined by the change in storage moduli. The temperature was set to 30 °C, the frequency was 1.5 Hz, and the gap between the parallel plates was 1 mm. During 500 s of UV irradiation, the change in the storage modulus was detected using a PP20 sensor.

2.3.3. Gel content

The gel contents of the cured acrylic PSAs after mixing with AlAcA were measured. Firstly, the sample weight was measured before 24 h immersion in toluene at room temperature (W_0).

The immersed sample was filtered through a 200 mesh wire net and oven dried at 70 °C for 24 h. The weight was then measured (W_{24}). The gel content was estimated using the following equation.

$$\text{Gel content } (\%) = W_{24}/W_0 \times 100$$

2.4. Characterization of the acrylic PSAs

2.4.1. Differential scanning calorimetry

The glass transition temperatures of the acrylic PSAs were determined by DSC (Q-1000 TA Instrument, USA). The samples were scanned twice from −80 to 200 °C, at a heating rate of 10 °C/min. In this analysis, the glass transition temperature of the acrylic PSA was detected from the second scan, excluding the thermal history effects.

2.5. Adhesion performance

The prepared acrylic PSAs films were attached to a stainless steel substrate, and rolled over twice using a 2 kg rubber roller. The sample was left to stand at room temperature for 24 h, and the 180° peel strength was measured using a Texture Analyzer (TA-XT2i, Micro Stable Systems, UK). The test speed was 300 mm/min, and the average peel strength was determined from five measurements. On the TA (XT2i, Micro Stable Systems, UK), the probe tack was measured using a 5 mm diameter stainless steel cylindrical probe. The test speed of the probe was 0.5 mm/s, the probe was placed in contact with the surface of the PSAs for 1 s with a constant pressure of 100 g/cm^2, and debonded at a 0.5 mm/s speed. The probe tack was estimated as the maximum debonding force. The shear adhesion failure temperature (SAFT) was measured using a 25 mm × 25 mm sized sample, which was attached to a stainless steel substrate by rolling twice with a 2 kg rubber roller. After loading with a 500 g weight, the samples were held in the oven at a heating rate of 0.4 °C/min, and the temperature when shear failure occurred was determined.

2.6. Optical properties

2.6.1. UV–visible spectroscopy

UV–visible spectroscopy (UV-1650PC Shimadzu, Japan) was used to examine the transmittance of the acrylic PSAs. Both the bare PET for the control and the acrylic PSA sample, which was coated on the PET film, were set on the instrument. The transmittance was determined in the visible range of 380–700 nm.

2.6.2. Prism coupler

The refractive index of the acrylic PSAs coated on a PET film was detected using a prism coupler 2010/M (Metricon, USA). The acrylic PSAs were UV-cured with a 1000 mJ/cm^2 intensity, after coating the pre-polymers on the PET film to produce PSA films without cohesive failure. A bare PET film was used as the reference. The prism and film were joined, and the incidence angle of the laser beam was varied, so the refractive index in both the thickness and plane directions could be determined.

3. Results and discussion

3.1. Photo-polymerization behavior of pre-polymer

3.1.1. Viscosity

The viscosity of the mixture increased sharply when a mixture of the monomers was polymerized with a UV light source. In the liquid state, the mixture was unable to coat the surface, but after polymerization, the mixture transformed into a semisolid phase that could be used as a coating. However, it would be very difficult to coat the surface if the viscosity is >50,000 or <100 cP. This is because a high viscosity makes it difficult to make a coating and a low viscosity means a lack of cohesion.[10] Therefore, the viscosity of the pre-polymer should be within 100–3000 cP. Table 1 lists the composition of each pre-polymer and Figure 1 shows the viscosity of each pre-polymer. In addition, the viscosity of the pre-polymer increased with increasing PEA content. This is because the glass transition temperature of PEA and 2-EHA is −22 and −70 °C, respectively. Therefore, the total T_g and viscosity of the pre-polymer increased with increasing PEA content.

3.1.2. RTIR spectroscopy

The photo-polymerization behavior of the pre-polymer was analyzed by RTIR. This measurement examines the change in the specific peak during UV irradiation. In this study, during photo-polymerization, the C=C double bond in each monomer converted to a C–C single chain, to form a polymer chain. In a previous study, the absorption peak at 810 cm^{-1} revealed the twisting of the C=C bond of the acrylic groups.[11] Therefore, the conversion behavior of

Table 1. Monomer compositions of the pre-polymers.

	PEA0	PEA25	PEA45	PEA75
2-EHA	95	70	50	20
PEA	0	25	45	75
AA	5	5	5	5
TPO	0.1	0.1	0.1	0.1

Note: All the monomers and a photoinitiator were based on the weight percent.

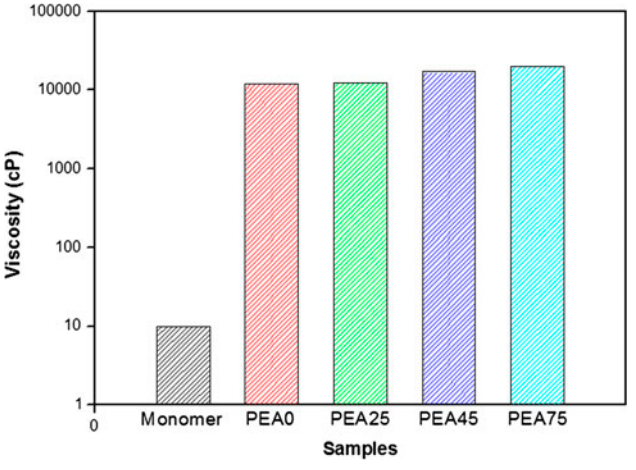

Figure 1. Changes in the viscosity of each pre-polymer by photo-polymerization.

the monomer after UV irradiation can be detected by observing the absorption peak at 810 cm^{-1}.[12] Figure 2(a) shows the three-dimensional decrease in the peak intensity of 2-EHA near 810 cm^{-1} over a short time interval. This suggests that the C=C bond of 2-EHA was decreased by UV irradiation for 600 s. As shown in Figure 2(b), the conversion of C=C groups before and after 600 s UV exposure was processed, and a relative decrease in 2-EHA occurred. In Figure 2(c), the cross section at 810 cm^{-1} of 2-EHA and PEA as a function of time indicates the relative concentration of each remaining monomer. Both monomers showed a rapid decrease in absorbance under 50 s, with a slow decrease to 0 thereafter. This shows that photo-polymerization occurred in very short time, i.e. a few seconds. PEA showed a faster reduction in the initial stage than 2-EHA. This demonstrates the faster reaction that occurs when the PEA content is increased to prepare the pre-polymer. When the PEA content was >75%, the pre-polymer could not be synthesized, due to rapid gelation. These phenomena also can be explained by the RTIR results.

3.1.3. Photo-differential scanning calorimetry

Photo-differential scanning calorimetry (photo-DSC) experiments were performed at the same temperature and light intensity, 25 °C and 70 mW/cm^2, to examine the photo-polymerization behavior of 2-EHA and PEA. The photo-DSC profiles were used to determine the photo-polymerization kinetics and reaction rate.[12] In the case of free radical polymerization, the maximum peak of the thermogram was achieved directly after the light was turned on. Figure 3(a) and (b) shows the photo-DSC thermograms of 2-EHA and PEA, and the integrated area under the thermogram curves, respectively. The thermograms of the two samples showed an immediate increase in peak intensity, followed by a decrease to 0 W/g. The 2-EHA showed a lower peak of heat flow than PEA. This indicates that PEA is more reactive than 2-EHA, because the peak height and total area under the thermogram curve of PEA was larger than that of 2-EHA. Moreover, the incident slope of PEA at 0.5 s was steeper than that of 2-EHA. From these results, the photo-polymerization reactivity of the 2-EHA and PEA mixture increased with increasing PEA content. Moreover, the viscosity of the pre-polymer synthesized from the 2-EHA and PEA mixture increased with increasing PEA content. A pre-polymer containing 95% PEA could not be synthesized, due to the high reactivity of PEA, and the high viscosity after a rapid reaction.

3.2. UV-curing behavior of acrylic PSAs

3.2.1. Modular advanced rheometer system

Figure 4 shows the viscoelastic changes in the acrylic PSAs as a function of the PEA content. After a damping period without UV-curing, Figure 4 shows the increase in the storage moduli with increasing UV-curing time. The change in the storage moduli increased suddenly, and remained steady. This indicates that the monomers remaining in the pre-polymer reacted directly from the start of UV irradiation. In addition, the storage moduli of the acrylic PSAs increased with increasing PEA content. This is because the curing speed of PEA is faster than that of 2-EHA. Therefore, the rates of conversion by UV-curing also increased with increasing PEA content. Moreover, the increase in PEA content affected the increase in storage moduli, due to the high conversion and high T_g.

3.2.2. Gel contents

The gel contents were calculated, to determine the degree of curing of acrylic PSAs, by measuring the insoluble material remaining.[13] The gel content increased gradually after

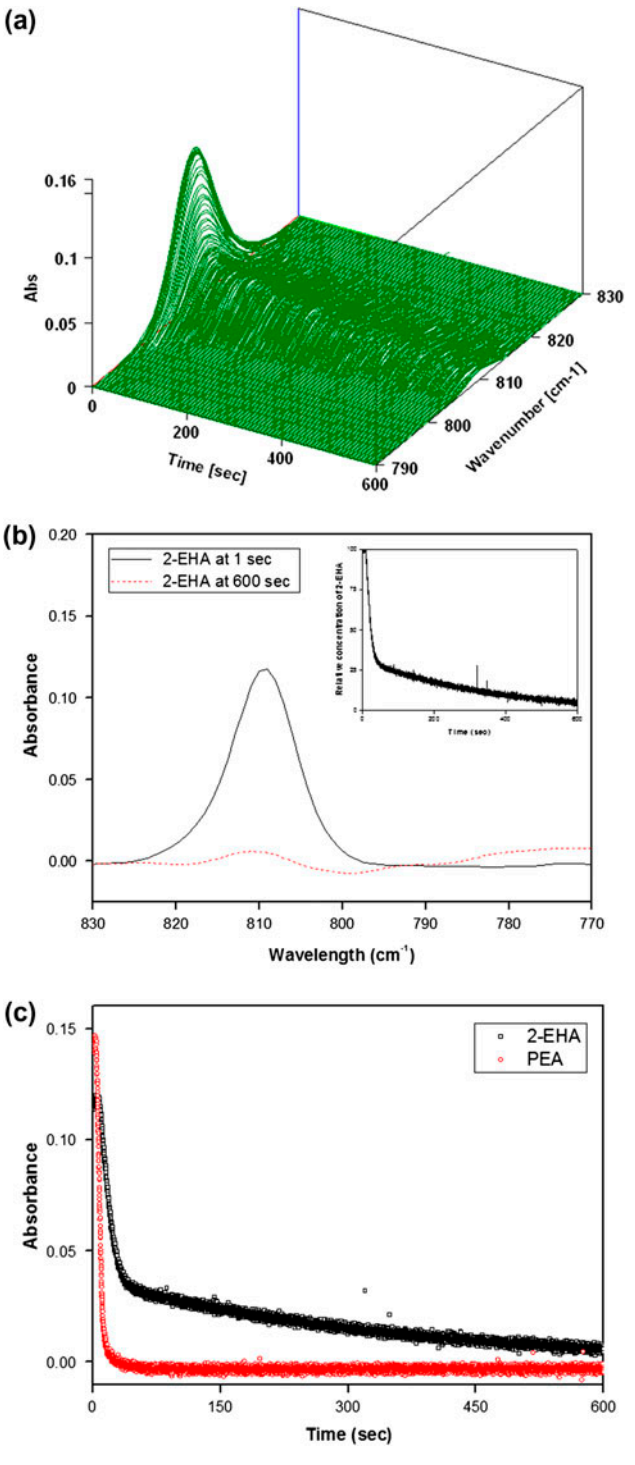

Figure 2. (a) Three-dimensional RTIR spectra of 2-EHA during 600 s UV irradiation; (b) FTIR spectra of the 2-EHA before and after 600 s UV irradiation, with inset showing the decrease in the relative 2-EHA concentration during photo-polymerization; and (c) cross section spectra of 2-EHA and PEA at the 810 cm^{-1} peak.

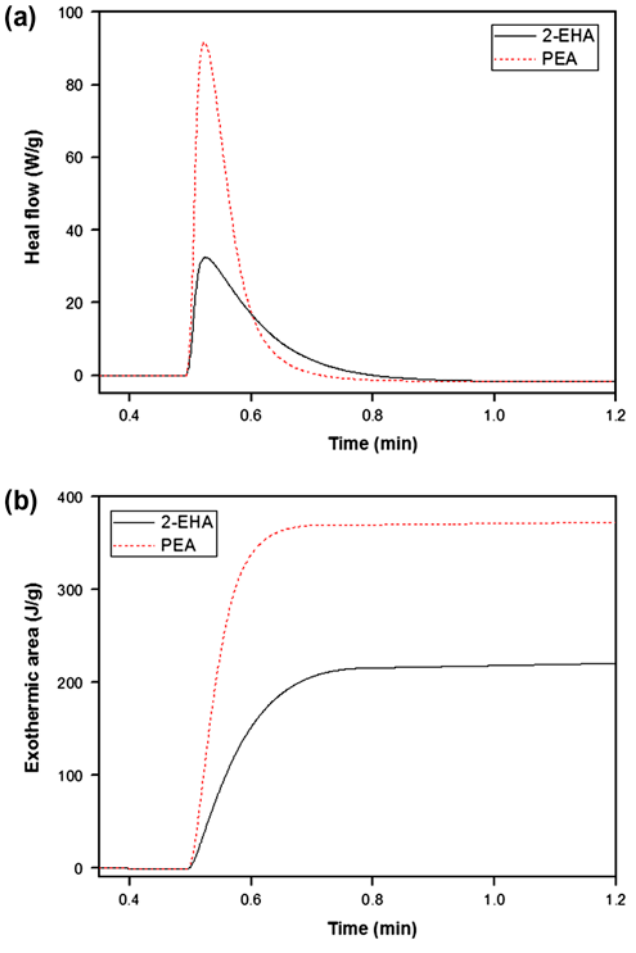

Figure 3. (a) Photo-DSC thermograms and (b) integrated area under curve of 2-EHA and PEA containing 0.1 wt.% of TPO.

curing the acrylic PSAs by UV irradiation and AlAcA, as shown in Figure 5. The gel contents also increased with increasing UV dose. However, the rate of increase was decreased by increasing the UV dose. In addition, the standard deviation of the gel contents decreased considerably at a UV dose of 1000 mJ/cm^2. This suggests that almost all the acrylic PSA samples were cured well at a UV dose of 1000 mJ/cm^2. AlAcA was added at the same amount to all acrylic PSA samples, to crosslink the acid group of the acrylic PSAs. Without the UV irradiation, there was only a small concentration of gel present.

3.3. Characterization of acrylic PSAs

3.3.1. Differential scanning calorimetry

The glass transition temperatures of acrylic PSAs are influenced by the monomer composition. The T_gs of the acrylic PSAs were measured by DSC. As shown in Figure 6(a), the T_gs of the acrylic PSAs increased slightly after UV-curing. This suggests that the acrylic PSAs formed a larger network structure after UV-curing. In addition, T_gs of the acrylic PSAs

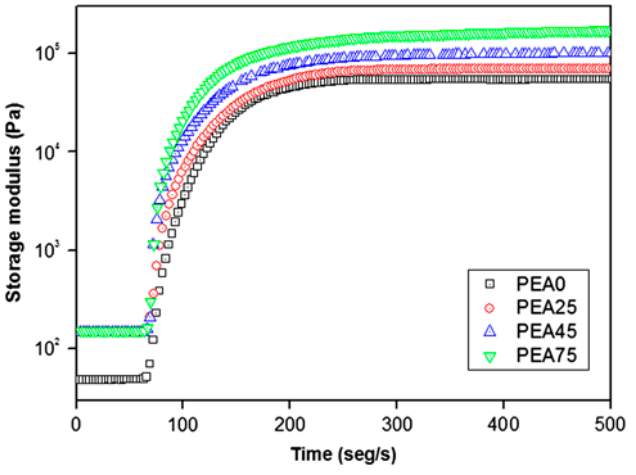

Figure 4. Change in the storage moduli, after UV-curing the acrylic PSAs with different PEA contents.

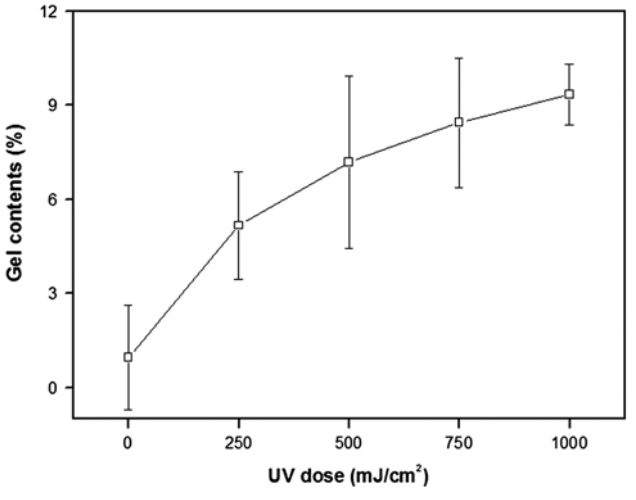

Figure 5. Gel contents of acrylic PSAs as a function of the UV dose.

increased considerably with increasing PEA content, because the T_g of PEA is higher than that of 2-EHA. Moreover, the PEA content had greater influence on the T_gs of acrylic PSAs than the degree of curing.[14]

3.4. Adhesion performance

The adhesion performance of acrylic PSAs, such as the peel strength, probe tack, and SAFT, was influenced by the UV dose and PEA content. The change in the glass transition temperatures of acrylic PSAs and crosslinking densities affected by UV-curing, are important factors for controlling the adhesion performance.[15]

To begin with, as shown in Figure 7(a), the peel strength of PEA45 decreased with increasing UV dose. In particular, at a UV dose <500 mJ/cm^2, cohesive failure occurred when

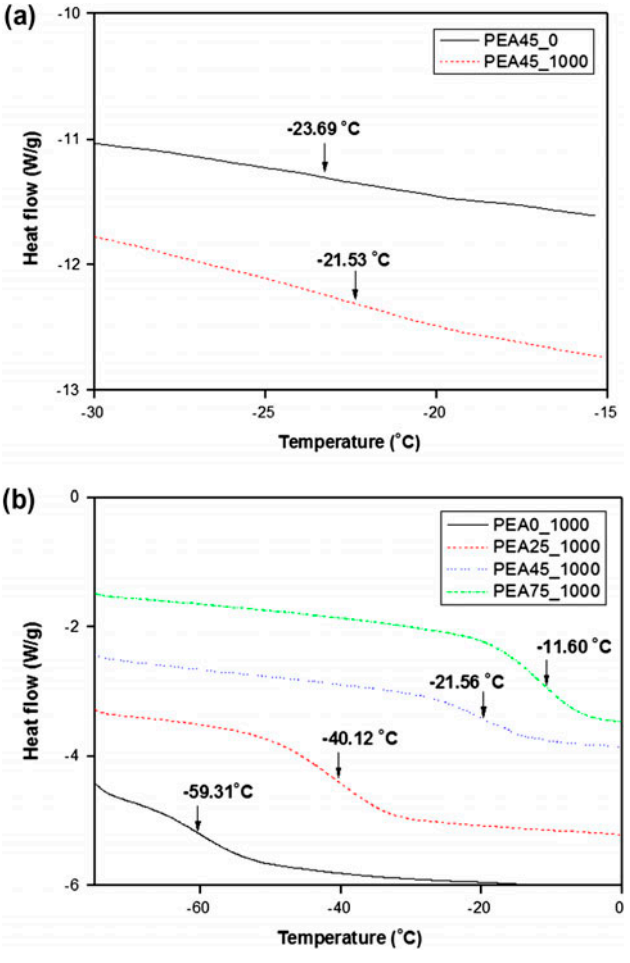

Figure 6. DSC thermogram and T_g of the acrylic PSAs (a) before and after UV-curing and (b) with variation of PEA contents.

the acrylic PSA sample was detached from the steel use stainless (SUS) surface. However, at a UV dose >750 mJ/cm^2, the acrylic PSA sample did not show cohesive failure, and the standard deviation of the samples was constant. The probe tack also decreased slightly with increasing UV dose. When the UV dose was <500 mJ/cm^2, fibrillation occurred between the stainless steel probe and acrylic PSAs. This is because with increasing UV dose, the acrylic PSAs showed greater cohesion force to endure the peeling stress and probe tack force. The cohesion force also increased slightly in the case of SAFT. This indicates that the cohesion force of acrylic PSA to endure a temperature change increases with increasing UV dose.

The PEA contents also affected the adhesion performance, as shown in Figure 7(b). In particular, in the case of the peel strength and SAFT, there was more change in adhesion than the probe tack. The standard deviations of the peel strength increased considerably with increasing PEA content. This suggests that a greater PEA content has more affinity to attach to the SUS surface, and the T_g increases with increasing PEA content. Acrylic PSA with a high T_g produced a more rigid structure, resulting in a higher peel strength. In addition, the storage moduli of acrylic PSAs also increased with increasing PEA content. In the case of the

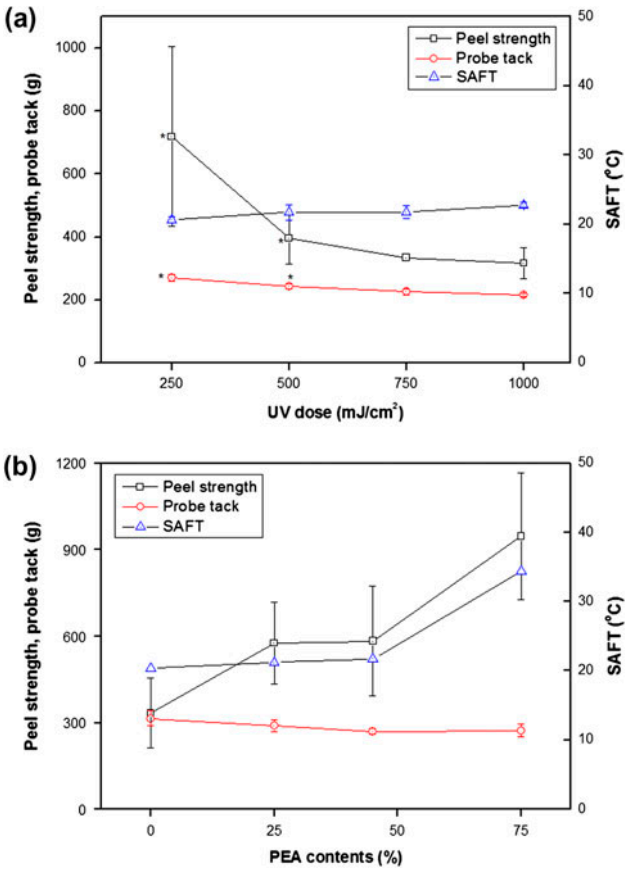

Figure 7. (a) Peel strength, probe tack, and SAFT of PEA45 as a function of the UV dose and (b) acrylic PSAs with UV-curing under 1000 mJ/cm^2 as a function of the PEA content (*cohesive failure).

probe tack, there was a slight decrease with increasing PEA content. The phenoxy group in the PEA monomer also affected the increase in SAFT and thermal resistance.

3.5. *Optical properties*

3.5.1. *UV–visible spectrometer*

The transmittance of each acrylic PSA sample was measured by UV–visible spectroscopy. The samples should show high transmittance (>95%), in order to be used in optical films.[16] In this study, the acrylic PSAs were coated on a PET film. Hence, the bare PET film was used as the reference. As shown in Figure 8, the transmittances of all acrylic PSAs were >95%, demonstrating high transparencies in the visible wavelength.

3.5.2. *Prism coupler*

Figure 9 shows the refractive index of acrylic PSAs in the visible range. The refractive indices of the acrylic PSAs increased with increasing PEA content in the visible range. In particular, between 500 and 600 nm, the refractive indices of PEA45 and PEA75 were much

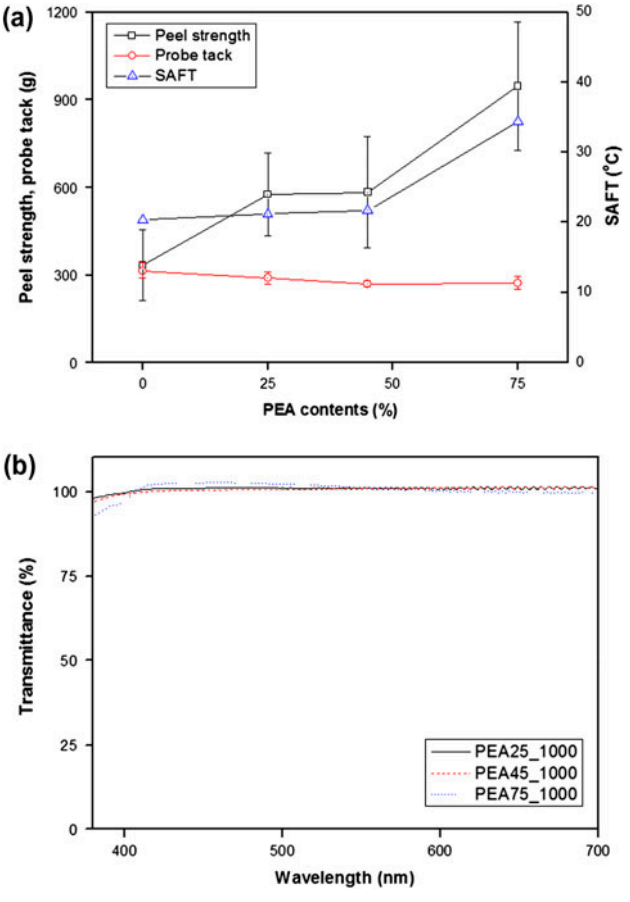

Figure 8. Transmittance of acrylic PSAs in the visible area, 380–700 nm with the (a) increment of UV dose and (b) increment of PEA contents.

higher than that of PEA 25. This illustrates the effect of the PEA content, which increased the refractive index of the polymer, due to the presence of a phenyl group.[9] PEA is a high refractive index monomer, with a refractive index of 1.518. Generally, the refractive index of a polymer containing a high refractive index functional group is higher than that of the monomer. In this manner, acrylic PSAs with >45% PEA had high refractive indices >1.55 in the visible range. The refractive index is dependent on the wavelength, with the real part of the refractive index decreasing with increasing wavelength. In this regard, PEA affected the increase in refractive index, particularly in the 500–600 nm wavelength.

4. Conclusions

Acrylic PSAs with different PEA concentrations were photo-polymerized and UV-cured. The photo-polymerization behavior of the pre-polymer was monitored by the change in viscosity, RTIR, and photo-DSC. The reactivity of PEA was >2-EHA. Therefore, the rate of conversion was also high. Moreover, the viscosity of the pre-polymer increased with increasing PEA content, because of the higher T_g of PEA than 2-EHA. The curing behavior of the acrylic

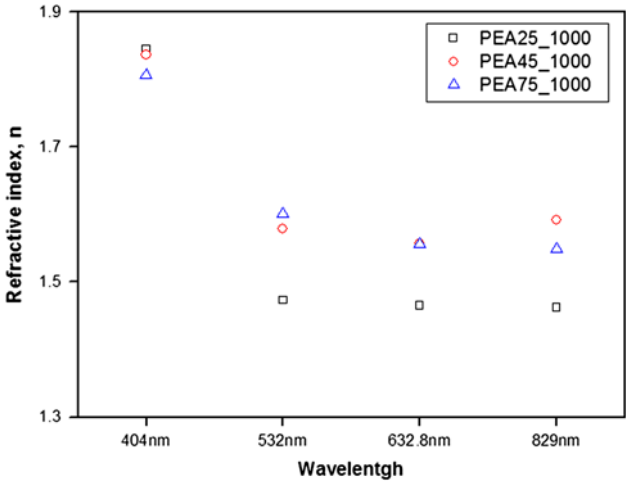

Figure 9. Refractive indices of the acrylic PSAs with different PEA contents.

PSAs was examined using shrinkage test, Modular advanced rheometer system (MARS), and gel content measure. The change in shrinkage was not precisely determined, due to the relaxation ability of the acrylic PSAs. The storage moduli increased with increasing UV-curing time and PEA content. The gel contents of the acrylic PSAs also increased with increasing UV-curing dose. This is because the conversion of the remaining monomer into a polymer produced a rigid structure. The adhesion performance was measured by peel strength, probe tack, and SAFT. The peel strengths of the acrylic PSAs decreased with increasing UV dose and increased with increasing PEA content. The probe tacks decreased slightly with increasing UV dose and PEA content. SAFTs increased slightly with increasing PEA content. The PEA content had a larger effect on improving the optical properties, than did the UV dose. The transmittances of the acrylic PSAs with <75% PEA were >95%. The refractive indices of the acrylic PSAs increased with increasing PEA content, due to its high refractive index, >1.5, which affected the overall refractive indices, particularly in the visible region.

References

[1] Yang HWH. Water-based polymers as pressure-sensitive adhesives-viscoelastic guidelines. J. Appl. Polym. Sci. 1995;55:645–652.
[2] Chang EP. Viscoelastic windows of pressure-sensitive adhesives. J. Adhes. 1991;34:189–200.
[3] Kano Y, Akiyama S. Poly(butyl acrylate)/poly(vinylidene fluoride-co-hexafluoroacetone) blends as pressure-sensitive adhesives. J. Appl. Polym. Sci. 1997;63:307–313.
[4] Kim HJ, Mizumachi H. Miscibility and peel strength of acrylic pressure-sensitive adhesives: acrylic copolymer-tackifier resin systems. J. Appl. Polym. Sci. 1995;56:201–209.
[5] Tse MF. Studies of triblock copolymer-tackifying resin interactions by viscoelasticity and adhesive performance. J. Adhes. Sci. Technol. 1989;3:551–570.
[6] Czech Z. Crosslinking of pressure sensitive adhesive based on water-borne acrylate. Polym. Int. 2003;52:347–357.
[7] Schwalm R. UV coatings – basics: recent developments and new applications. Amsterdam: Elsevier Science; 2007.
[8] Chang EP, Holguin D. Electrooptical light-management material: low-refractive-index adhesives. J. Adhes. 2005;81:925–939.
[9] Miyamoto M, Ohta A, Kawata Y, Nakabayashi M. Control of refractive index of pressure-sensitive adhesives for the optimization of multilayered media. Jpn J. Appl. Phys. 2007;46:3978–3980.

[10] Piglowski J, Koziowski M. Rheological properties of pressure-sensitive adhesives: polyisobutylene/sodium carboxymethylcellulose. Rheol. Acta. 1985;24:519–524.
[11] Do HS, Park JH, Kim HJ. UV-curing behavior and adhesion performance of polymeric photoinitiators blended with hydrogenated rosin epoxy methacrylate for UV-crosslinkable acrylic pressure sensitive adhesives. Eur. Polym. J. 2008;44:3871–3882.
[12] Tauber A, Scherzer T, Weib I, Mehnert R. UV curing of a pressure sensitive adhesive coating studied by real-time FTIR spectroscopy and laboratory scale curing experiments. J. Coat. Technol. 2004;74:41–47.
[13] Do HS, Park YJ, Kim HJ. Preparation and adhesion performance of UV-crosslinkable acrylic pressure sensitive adhesives. J. Adhes. Sci. Technol. 2006;20:1529–1545.
[14] Joo HS, Park YJ, Do HS, Kim HJ. The curing performance of UV-curable semi-interpenetrating polymer network structured acrylic pressure-sensitive adhesives. J. Adhes. Sci. Technol. 2007;21:575–588.
[15] Joo HS, Do HS, Park YJ, Kim HJ. Adhesion performance of UV-cured semi-IPN structure acrylic pressure sensitive adhesives. J. Adhes. Sci. Technol. 2006;20:1573–1594.
[16] Chau JLH, Lin YM, Li AK, Su WF, Chang KS, Hsu SLC, Li TL. Transparent high refractive index nanocomposite thin films. Mater. Lett. 2007;61:2908–2910.